PERFORMANCE OF PRINTABLE ANTENNAS WITH DIFFERENT CONDUCTOR THICKNESS

A DISSERTATION

Submitted in partial fulfillment of the requirements for the award of the degree of

MASTER OF TECHNOLOGY

in

ELECTRONICS AND COMMUNICATION ENGINEERING

(With Specialization in RF and Microwave Engineering)

By

ARUN KUMAR SOWPATI

DEPARTMENT OF ELECTRONICS AND COMPUTER ENGINEERING
INDIAN INSTITUTE OF TECHNOLOGY ROORKEE
ROORKEE -247 667 (INDIA)

OCTOBER, 2009

CANDIDATE'S DECLARATION

I hereby declare that the work, which is being presented in the dissertation entitled, **"Performance of printable antennas with different conductor thickness"**, which is submitted in the partial fulfillment of the requirements for the award of degree of Master of Technology (**M.Tech)** in **RF and Microwave Engineering,** submitted in the Department of Electronics and Computer Science Engineering, **Indian Institute of Technology – Roorkee**, Roorkee (INDIA), is an authentic record of my own work carried out under the guidance of Professor Heli Jantunen, Microelectronics and Material Physics laboratory, University of Oulu, Finland and Professor M.V.Kartikeyan, Department of Electronics and Computer Engineering, Indian Institute of Technology, Roorkee.

I have not submitted the matter embodied in this dissertation for the award of any other degree or diploma.

Dated : 09/09/2009

Place: Roorkee

S. Arun Kumar

(Arun Kumar Sowpati)

CERTIFICATE

This is to certify that the above statement made by the candidate is correct to the best of my knowledge.

Heli Jantunen, prof.

UNIVERSITY OF OULU
Microelectronics Laboratory
Finland

(Dr. Heli Jantunen)
Professor
Microelectronics and Material Physics laboratory,
University of Oulu ,
Finland.

(Dr. M.V.Kartikeyan)
Professor
Dept. of E & C Engg.
IIT-R, Roorkee – 247667,
INDIA

ABSTRACT

This thesis investigated the optimum conductor thickness required for an inkjet printed L-shaped monopole antenna operating in the 2.4 WLAN (2.4 – 2.484 GHz) band for achieving a comparable antenna performance with a reference antenna made with copper metallization. The antenna performance, namely total antenna efficiency, is used to make comparison between the inkjet printed and reference antennas. The computer aided design of the antenna is performed through Ansoft HFSS (High Frequency Structure Simulator), a commercial 3-D (dimensional) electromagnetic simulator. The results offer knowledge how flat antennas with optimized performance can be designed and fabricated by inkjet printing without excessive use of ink.

Design, modeling and measurements are performed in the Microelectronics and Materials Physics laboratory, University of Oulu. The antennas with different silver layer thickness were printed using an ink-jet printer in the Institute of the Electronics, Tampere University of Technology. Polyphenylene Sulfide (PPS) was used as a substrate material for the antennas and conductive areas were printed with a commercial nano silver ink. Measurements included RF characterization, total antenna efficiency, gain and radiation pattern measurements.

The results show that with 5.5 μm thickness of inkjet printed nano silver ink antenna achieved comparable antenna performance to reference antenna made of Rogers 4003c copper laminate thickness about 20.5 μm.

Key words: Antenna, 2.4 GHz, wireless telecommunication, printed electronics.

ACKNOWLEDGEMENTS

This Master's Thesis has been made at Microelectronics and Material Physics laboratories, University of Oulu, during 2009. This work is part of DemoPrint project related to printable electronics and studied the performance of printable antennas with different conductor thickness.

I would like to thank the supervisors of my thesis Professor Heli Jantunen and Professor M.V. Kartikeyan for all advices and guidance during this work. I am grateful to researcher Vamsi Krishna Palukuru for the help he have gave me throughout the course of this thesis. I would also thank Dr.-Ing. Jagadish C. Mudiganti and Mr. Ashwini Arya, Research Scholar, Department of Electronics and Computer Engineering for their kind help and support.

Table of contents

1.INTRODUCTION

Printable electronics is a new area of research and development of electronics manufacturing technique using commercial printing processes. When the technology matures it will have a capacity to deliver very large amounts of printed electronic units at a very favorable price, as compared to traditional silicon based technology. It is a production process for low cost future electronic devices and components. It decreases the manufacturing costs and allows design of new flexible, non-planar, even three-dimensional (3-D) structures with inhomogeneous substrate materials [1-5]. Printed antennas can offer a variety of beneficial properties including conformability, compactness.

Printed antennas are one of the most potential applications of printable electronics. The performance of the antenna (gain, radiation efficiency etc.) also in the case of printed ones depends on the antenna type, its environmental issues and properties of the materials and manufacturing technique used. An important factor when we talk about printed antennas is the properties of the printed conductive areas. Electrical properties of the ink are mostly determined by conductive particles mixed and how they are interconnected after curing. However the thickness of the printed conductive layer plays an important role on antenna performance [2-3]. The printed conductor thickness of the antenna should be several times greater than the skin depth at its operating frequency in order to have higher efficiency of the antenna [5]. Radiation properties of antennas depend on the conductivity of the metal printed, conductor thickness, surface roughness [5]. However the inkjet printing provides very thin layers even less than 1 μm and enables an efficient utilization of the ink [4] and thus sequential printing of a number of thin layers is needed. This can effect on the accuracy of the conductive lines. Additionally the inkjet printed lines have greater losses than the etched line due to their smaller electrical conductivity because of mixing silver particles with ink additives. Hence, conductivity of silver ink is low compared to bulk silver conductivity. Printing of too thick conductive layers should be also avoided since the accuracy of lines further deceases and excess consumption of the ink quickly increases the material costs. The possibility of minimizing the amount of ink used to print the antenna by printing thick layer only in places of higher current density was reported previously [2]. However, there has been no

systematic investigation on the impact of the increase of printed layer thickness on antenna performance reported.

In this thesis work, the impact of the inkjet printed silver layer thickness on the performance of a L-shaped monopole antenna operating in 2.4 WLAN (Wireless Local Area Networks) frequency band (2.4 – 2.484 GHz) is investigated. The antenna is designed using Ansoft High Frequency Structure Simulator (HFSS, Version 11.1), a commercial electromagnetic simulator. A reference antenna made of Rogers 4003C copper laminate was also fabricated to compare its performance to the performance of the ink-jet printed one. At the end of the thesis the results are discussed with possible future actions.

1.1. Literature survey:

Rida and Vyas (2008) presented a paper based wireless sensor module, a wifi antenna on paper via, and a paper based three dimensional RFID antennas. These modules prove paper and inkjet printing as a candidate for the first ultra low cost paper based wireless electronics. A very low cost substrate, paper makes one of the best substrate candidates for applications of Radio Frequency Identification (RFID), wireless and ubiquitous sensing due to the fact that it is the lowest cost materials, having good flexibility, minimal water absorption if treated with an appropriate coating and is suitable for fast printing processes such as direct write methodologies instead of the traditional metal etching techniques [1].

Siden and Fein (2007) investigated the possibility of minimizing the amount of ink used per antenna. This can be achieved by printing thicker ink layers, where the antenna structures have high current density. Two antenna structures (Dipole, Bow-tie) had taken and characterize the influence of the variable-layer-thickness in antenna printing. The main result is radiation efficiency depends primarily on the amount of ink used for printing the antenna [2].

Li and Vyas (2007) designed and fabricated a UHF RFID tag module using inkjet printing technology. The use of inkjet printing process in the development of multilayer RF structures on a paper substrate has been demonstrated and proved that paper based inkjet-printing is a very low cost, simpler and faster fabrication [3].

Siden and Nilsson (2007) studied the limitations in a minimum line width for flexographic, screen and inkjet printed RFID antennas. Inkjet process provides very thin lines whose thickness is less than 1 μm a sheet resistance of approximately 50 Ω/□ was achieved when printed on a 100 μm thick transparency film. Line width of 2 mm provide efficient antennas [4].

Matti and Pauliina (2007) designed and manufactured a transmission line and a patch antenna for 2.4 GHz ISM band. The printed lines have greater losses than the etched line due to their thinner profiles and smaller electrical conductivity. Thickness of the metals should be several times greater than the skin depth. Radiation properties of antennas depend on the conductivity, antenna thickness, surface roughness, and antenna geometry [5].

Rida and Tentzeris MM (2007) investigated inkjet printed antennas on paper based substrates. Two EM methods (Cavity Resonator and TL methods) were utilized for the characterization of and tanδ respectively. An RFID tag prototype module using stubs for matching to the IC on paper-based substrates operating in the UHF frequency band was designed [6].

Marko and Niina (2005) characterized the conductor line properties for different substrates: resistance, yield as a function of line width, coil inductance, folding endurance, adhesion, printed antenna properties and maximum current density. A printed resistance down to 50 mΩ / □ was obtained, with conductor lines 4-7 μm [7].

Andrei and Peter (2003) designed and fabricated Bow-tie antennas using screen printing technique. Conductive layers of paint with limited conductivity have to be sufficiently thick in order to achieve high radiation efficiency. With conductive layers of thickness beneath 10 μm, silver-based paint with finite conductivity showed low radiation efficiency at high frequency. Thickness above 30 μm closely resembled radiation characteristics for perfect conductor antennas. Only Ink-jet technologies allowing printing multiple thin conductive layers with relatively low edge roughness [8].

Sari and Leena (2007) printed silver ink bowtie RFID antennas on paper substrates. Screen printing were used to produce prototype Bow-Tie tags. The maximum reliable read ranges of the tags were measured thorough stacked paper and also in air. The analysis and functioning of the antenna design are also discussed. All inks and paper substrates were suitable as antenna material and the prototype tag antennas had good reading performance. The maximum reliable read ranges were quite the same as for copper and aluminum tags [9].

Li and Rida (2007) presented novel design and integration approaches for improving the performance UHF Radio Frequency Identification (RFID) tags with embedded power source. Inkjet printing on Ultra-low-cost organic substrates are investigated for the UHF frequency band. It enable the low cost and large-scale implementation of RFID-enabled semiautonomous sensors for "cognitive-intelligence" applications. The use of embedded rechargeable thin film batteries will increase the tag's lifetime. This technology could potentially revolutionize sensor nodes and RFID tags for security, logistics, automotive and pharmaceutical applications [10].

Gunter and Petersen designed and integrated printed antennas in plastic body parts of automotives for reception of electromagnetic waves such as AM/FM, GSM. The antennas are printed on plastic films which are transferred to the plastic body parts. Antenna and 3-D designs completely integrated in the plastic part. The performance and comaptatibility of the materials testing described. Applications in cars and agricultural vehicles described [11].

Jolke, Patrick and Ervin (2009) experimental study on the spreading of inkjet printed droplets of a polystyrene/toluene solution with varied molar masses on solid dry surfaces. The relative errors between experimental data and the models were between 2 and 20%. Inkjet printed droplets of a polystyrene solution the spreading on the substrate after impact strongly depends on the polymer's molar mass due to its influence on the viscosity [12].

Tentzeris and Rida presents design and development of RFID and RFID-enabled sensors on flexible low-cost substrates for the UHF band and up to microwave frequencies. Demonstrated design and fabrication of antennas, integration with ICs and microcontrollers, power sources, as well as ink-jet printing techniques. Focus on the "first green RFID-enabled sensor", battery-less long-range RFID modules, and current problems in design/measurements of RFID-enabled sensors that make extensive use of power scavengers of renewable energy sources [13].

Sridhar and Akkerman tested adhesion between the printed component and the substrate. This is of paramount importance to inkjet printed electronics, as the interface between the substrate and the component is established purely by virtue of their atomic or molecular forces and energies, without the usage of a joining medium solder and glue. This describes the need for compatibility between the two entities. The thicknesses of the individual layers are less than 1μm and are susceptible to failure. Nevertheless, suitable peel testing methods are being developed to quantify the adhesion in the case of flexible substrates. Based on the test results, the parameters for the printing process will be tuned to obtain more robust components [14].

Eloi, Jordi and cristina studied different active and passive devices and implemented using inkjet printing in order to analyze printing problems and unknown effects due to materials and processes. RF frontend devices designed using inkjet technique on different flexible substrates as PET, Kapton and paper. Inductive coupling antennas, microwave-like-filters have been designed at different frequencies and using different substrates and printing processes [15].

Prabir, Paul and Steven Printed several patterns on the fabrics and plastic films have been carried out. Designed patterning of carbon nano tubeconducting polymer based electronic ink on a textile substrate by controlled micro-droplet deposition and its diffusion into the fabrics to design flexible antennas and antenna arrays in the microwave and millimeter wave frequency ranges. Developed a highly conducting nanotube based polymer conductive ink formulations alternative to silver for RFIDs. Measured such as gain vs. conductivity and impedance matching to establish the antenna principles in the materials [16].

Vamsi and Arto (2009) designed and presented inkjet printed inverted F-shaped antenna on a thin kapton substrate suitable for watch type wireless applications. The performance of printable antennas compared with a reference antenna made with copper. The effect of injet printed layer thickness and and impact of user's hand on antenna performance is experimentally studied. The shape of radiation pattern distorted due to proximity of user's hand [17].

Jolke and Mark (2009) studied dispersions on thin polymer substrates as a function of the antenna area and initial resistance. The presence of conductive antenna gives nanoparticle sintering in pre-dried ink lines. For dried nanoparticle inks connected to antennae, sintering times of 1 s are sufficient to obtain pronounced nanoparticle sintering and conductivities between 10 and 34% compared to bulk silver [18].

Shin and Lee (2008) discussed selection of ink and fabrication of printing process. Screen printed RFID antennas are compared with copper etched antennas. The developed silver nanopaste in the range of 20 to 50 nm without the inclusion of microparticles and flakes was sintered at 120 °C for 1 min, which is lower than that of conventional silver paste with microparticles and flakes, and its resistivity was found to be approximately 3 μΩ cm. The overall performance of printed RFID antennas with the developed silver nanopaste was found comparable to that of copper etched ones. The minimum required thickness of printed RFID antennas in the specified range is calculated in terms of skin depth [19].

Fernando and Hitoshi (2007) reported printed antennas using conductive ink on coated paper for RFID applications. Those antennas achieve high conductivity and low resistance suitable for RFID application. design a low-cost RFID antenna printed onto a textile-based substrate with inkjet technology, which enables the finer resolution in smaller application spaces with less materials, more than any other printing technologies, a direct method to precisely place materials onto the fabric in one step, and a continuous digital process to change outputs without intermediate stages. Textile-based antennas could be used to replace other materials currently utilized, such as Taslan [20].

1. 2. Motivation

Printed electronics is a new area of research producing low cost electronic devices suitable also for flexible substrates. This technology provides several manufacturing methods like inkjet, roll-to-roll or flexographic printing. Printed antennas have a variety of beneficial properties such as mechanical durability, conformability and compactness. Thus they can provide interesting options for both the military and commercial sectors. One application area is e.g. light, compact portable devices like mobile phones or wrist computers. Additionally it becomes more and more common to print tag antennas using electrically conductive ink for produced Radio Frequency Identification Tags (RFID) tags.

Inkjet printing, used in this work, is a direct material deposition method proposed to be one important manufacturing technique for future electronic devices. The challenge in this technique is however the ink itself and its printing. The first important issue is the electrical properties of the cured ink should be as close as possible to the properties of bulk silver or copper. The properties of ink are mostly determined by conductive (e.g. silver, copper) particles mixed into the ink solution and with commercial nano silver inks today conductivities like 2.5×10^7 S/m, 4.16×10^7 meters/m are available. The second challenge is the thickness of conductive lines available. It has been shown that silver based printed antennas with a thick enough printed conductor layer comparable efficiency as their corresponding copper antennas can be achieved [4]. In this thesis the main target is to research suitability of inkjet printing for L-shaped monopole antenna for 2.4 WLAN. Especial challenge is to optimize the thickness of printed silver line with the lower limit being related to the skin depth, and the upper to enable accurate structures without excess use of ink or any deterioration in antenna performance.

1.2. Objective and outline of the thesis

The thesis is divided into five chapters and organized as follows. Chapter 2 describes the basic antenna theory for understanding the fundamentals of antenna principles and results of antenna radiation properties discussed in thesis. In Chapter 3, the design of the antenna, substrate materials used in the antenna fabrication and their properties, parametric study of different geometrical variables affecting the performance of the antenna and inkjet printing process were investigated. Chapter 4 reports describes the simulation and fabrication of the L-shaped monopole antenna. It also shows the measurement results of the L-shaped monopole antenna. Finally the results are discussed and concluded in Chapter 5.

2. Performance parameters

To describe the performance of an antenna, definitions of various parameters are necessary. Parameter definitions useful for the thesis given in this chapter are described as follows.

2.1. Directivity and Gain

2.1.1 Directivity

One of the most important properties of an antenna is how much it concentrates energy in one direction in preference to radiation in other directions [21]. This characteristic of an antenna is called its directivity. The directivity defines the ratio of the radiation intensity (U) in a certain direction from the antenna to the average radiation intensity in overall direction. The average radiation intensity (U_{avg}) equal to the total power radiated by 4π. In mathematical form, it can be represented as

$$D = \frac{U}{U_{avg}} = \frac{4\pi U}{P_{rad}} \tag{1}$$

P_{rad} = total radiated power (W) directivity is solely determined by the radiation pattern of an antenna.

2.1.2 Gain

Gain of an antenna (G) is closely related to the directivity taking into account the efficiency of the antenna and its direction properties [21]. In mathematical form, it can be represented as

$$G = \frac{4\pi U_{\max}}{P_{in}} \tag{2}$$

$$P_{rad} = e_o P_{in} \tag{3}$$

$$G = e_o D \tag{4}$$

where e_o represents the total efficiency of an antenna. P_{in} = power accepted by the antenna.

2.2. Antenna efficiency and radiation efficiency

The total antenna efficiency takes into account of the reflection, conduction, and dielectric losses at the input terminals and within structure of the antenna. Those losses are (1) reflection losses due to mismatch between the transmission line and the antenna and (2) I^2R losses (conduction and dielectric). Overall efficiency can be written as

$$e_o = e_r e_c e_d \tag{5}$$

where e_o = total efficiency , e_r = reflection(mismatch) efficiency, e_c = conduction efficiency, e_d = dielectric efficiency [21].

The radiation efficiency is defined as the ratio of the power delivered to the radiation resistance R_r to the power delivered to R_r and R_l (load resistance).

$$e_{cd} = \frac{R_r}{R_r + R_l} \tag{6}$$

2.3. Return loss

Return loss is a measure of the effectiveness of power deliver from a transmission line to a load such as an antenna. If the power incident on the Antenna-Under-Test (AUT) is P_T and power reflected back to the source is P_R, the degree of mismatch between the incident and reflected power in the travelling waves is given by the ratio P_T / P_R. The higher power ratio is, the better the load and line are matched [23]. If the power transmitted by source is P_T and power reflected is P_R, then the return loss in dB is given by

$$RL(dB) = 10 \log_{10} \frac{P_T}{P_R} \tag{7}$$

2.4. Input Impedance and impedance matching

The input impedance of an antenna is the impedance presented by the antenna at its terminals. Thus, suitable terminals must be defined for an antenna. In many cases other objects and antennas will effect on the antenna input impedance and here it is assumed that the antenna is isolated. The input impedance is composed of real and imaginary parts

$$Z_A = R_A + jX_A \tag{8}$$

where R_A is input resistance and X_A is input reactance representing power stored in the near field of antenna. The input resistance R_A consists of two parts

$$R_A = R_r + R_l \tag{9}$$

where R_r is radiation resistance of the antenna and R_l is loss resistance of the antenna [21, 22]. As mentioned earlier the input impedance represents load in the end of the transmission line. If the impedance of load (Z_L) is different from the nominal impedance (Z_0) of transmission line, discontinuity in transmission exists and thus discontinuity reflection is formed. This reflection caused by miss matching of the antenna reduces the total power transferred to the antenna. In a perfectly matched case all the power is transferred to the antenna and $Z_L = Z_0$. The voltage reflection coefficient can be determined as

$$\rho_l = \frac{Z_l - Z_o}{Z_l + Z_o} \tag{10}$$

The voltage standing wave ratio (VSWR) can be defined with equation

$$VSWR = \frac{V_{\max}}{V_{\min}} = \frac{1+|\rho|}{1-|\rho|} \tag{11}$$

where V_{max} and V_{min} are the amplitudes of the maximum and minimum voltages of the standing wave in the transmission line and ρ is the reflection coefficient of the power.

2.5. Skin depth

Skin depth, or characterstic depth of penetration is defined as [24]

$$\delta = \frac{1}{\sqrt{\pi f \mu_o \mu_r \sigma}} \tag{12}$$

where μ_o = permeability of free space, μ_r = permeability of the medium,
σ = conductivity of the medium in S/m.
The amplitude of the fields decay by an amount 1/e or 36.8%, after traveling a distance of one skin depth.

2.6. Radiation pattern

Radiation pattern is a graphical representation of the radiation properties of an antenna as a function of space coordinates [10]. In most cases, the radiation pattern is determined in the far-field region and is represented as a function of the directional coordinates. Spherical polar coordinates are used to represent the radiation pattern of an antenna. The type of radiation pattern can vary from isotropic, via directional to omnidirectional pattern. Isotropic radiator is widely used as a reference due to its nature to be ideal, hypothetical lossless antenna having radiation equally in all directions. Directional antenna has property to radiate or receive electromagnetic waves more effectively in some directions than in others. Omnidirectinal pattern defined as having an non directional pattern in a given plane and a directional pattern in any orthogonal plane. Typical radiation pattern is seen in Fig. 1 with different types of lobes which are sub-classified as follow; major or main lobe, side lobe and back lobe. Radiation lobe is a portion of the radiation pattern bounded by regions of relatively weak radiation intensity. Major lobe is defined as a lobe containing the direction of maximum radiation. Any lobe other than the main lobe is called minor lobe [21].

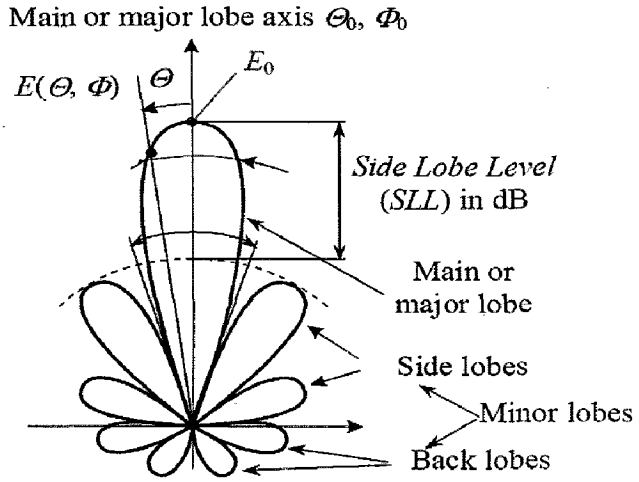

Fig. 1. Radiation lobes of an antenna pattern.

2.7. Field Regions

The electromagnetic field generated by an antenna to its surroundings is usually subdivided into three regions: reactive near-field, radiating near-field (Frensel) and far-field (Fraunhofer) [21]. These regions are designated according to each field structure, and there are a distinct difference between them even no abrupt changes in the field configuration are noted. These regions are shown in Fig.2.

The reactive near-field situates immediately surroundings the antenna, where reactive field predominates. Usually the outer edge of the reactive near field exists at a distance with radius of $R < 0.62\sqrt{d^3/\lambda}$ from the antenna surface, where λ is the wave length and d is the largest dimension of the antenna [21]. The radiating near-field is the region of the field between the reactive near-field and far-field. In this area the radiation field predominates and the angular field distribution is dependent upon the distance from the antenna. The inner boundary is taken to be the distance $R \geq 0.62\sqrt{d^3/\lambda}$ and the outer boundary the distance $R < 2d^2/\lambda$.

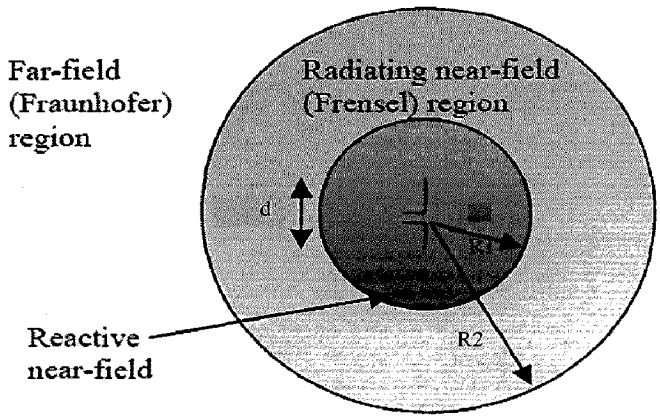

Fig. 2. Field regions of an antenna.

Fairfield (Fraunhofer) region is defined as that region of the field of an antenna where the angular field distribution is essentially independent of the distance from the antenna

If the antenna has a maximum overall dimension d, the far-field region is taken to exist at distances greater than $2d^2/\lambda$ from the antenna. An antenna focused at infinity, the far field region is referred to as the Fraunhofer region. In this region, the field components are essentially transverse and the angular distribution is independent of radial distance.

3. Inkjet printed L-shaped monopole antenna

In this chapter, L-shaped monopole antenna structure described. Ansoft HFSS (V.11) simulator has been used to model and simulate the L-shaped monopole antenna.

3.1. Antenna Structure

The geometry of the proposed ink-jet printed L-shaped monopole antenna on PPS (polyphenylenesulfide) substrate with dimensions of 20 x 5 x 1 mm^3 shown in Fig. 3. The antenna is soldered using silver paste on to 0.83 mm Rogers 4003C substrate serving as the ground. A ground opening of 28 mm x 10 mm is provided beneath the antenna to enable better antenna matching. A 50 Ω microstrip line is used as feed for the antenna. The total length of the antenna radiation strip is about 20 mm being about 0.163λ at 2.44 GHz operating frequency.

Ansoft High Frequency Structure Simulator (HFSS), a commercial three dimensional electromagnetic simulator was used for the design of the L-shaped monopole antenna.

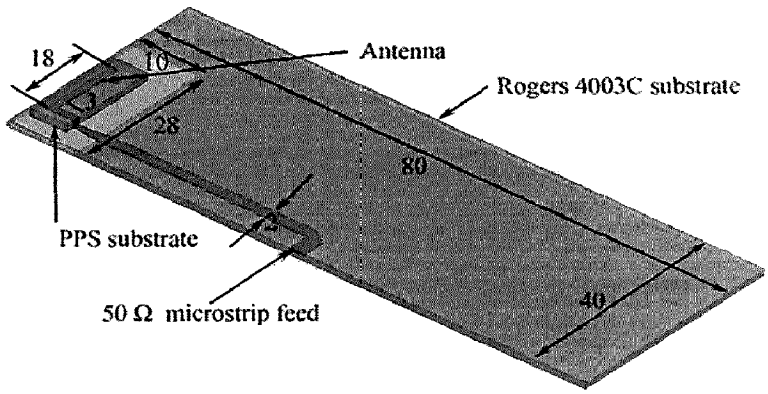

Fig. 3. Schematic diagram of the L-shaped monopole antenna on PPS substrate (dimensions in mm).

Ansoft HFSS is a high performance full-wave electromagnetic field simulator based on the Finite Element Method (FEM). It analyzes 3D and multilayer structures of general shapes. The design of MICs (Microwave Integrated Circuits), RFICs (Radio Frequency Integrated Circuits), patches antennas, wire antennas, and other RF/wireless antennas. It can be used to calculate and plot the S-parameters, VSWR,

current distributions as well as the radiation patterns. This FEM technique is very popular computational method for solving electromagnetic problems. It allows arbitrary geometries can be defined very easily with various levels of resolution in the problem space. The basic FEM formulation is closed box approximation and can include package effects [25]. In the design of the antenna, material parameters such as relative permittivity of PPS material which was used as substrate material for the antenna was considered to be about 3 for the purpose of simulation. The dimension of Rogers 4003C substrate (ε_r= 3.55) with ground plate was taken to be 80 mm x 40 mm. Conductive antenna structure to be printed with silver ink was designed on the top of the PPS substrate. The antenna was designed for 2.4 GHz WLAN band (2.4 – 2.484 GHz). Spacing between ground plane and antenna affects the impedance matching. The ground plane opening and the size of the antenna is optimized for a return loss below -10 dB across the 2.4 WLAN band. The prototype of the antenna was fabricated using 0.83 mm Rogers 4003C copper laminate with an approximate copper thickness of 20 μm. The measurements were promising and the second version of antenna was made with silver ink having conduciveness $\sigma = 3.38 \times 10^7$ Siemens/m and varying the conductor thickness of different layers.

The antenna was excited to resonate at 2.4 GHz frequency band. Fig. 3. shows the geometrical configuration of proposed Microstrip fed monopole antenna printed on PPS substrate with dielectric constant 3 and thickness 0.8 mm. The L-shaped monopole with dimensions 18mm and 3 mm to produce the resonant frequency 2.4 GHz. This antenna is attached to Rogers 4003 C substrate by hot pressing the upper substrate into desired dimensions and excited by microstrip line of width is 2 mm.

3.2. Substrate

Polymeres are low-cost materials with good chemical stability, mechanical strength, and flexibility, and they can be easily processed even into complex shapes. Polyphenylene sulfide (PPS) is semi crystalline thermoplastic polymer offering well-balanced characteristics like good flowablity, dimensional stability, electrical properties, and high temperature and chemical resistance [27]. This polymer is suitable for fast printing processes such as direct write methodologies instead of the

traditional metal etching techniques It has been used in commercially available film capacitors. It has also excellent high frequency properties like dielectric constant of 3 and loss tangent of 0.0001 at 1 MHz [28]. In this work the antenna is printed on one side of the PPS substrate and microstrip feed is on the Rogers 4003cc substrate has a dielectric constant of 3.55 and loss tangent of 0.0027 at 10 GHz [26].

3.3. Inkjet printing process

Printing technique is an efficient way to produce text and images. Benefits of printing processes are high speed fabrication i.e high volume products, low cost, flexible substrates, established technology and waste reduction. The main printing processes are offset lithography, flexography, gravure, screen printing, electro photography and inkjet printing. Requirements for printing electronic components are accuracy of position, amount of material deposited and resolution. Ink jet is the most developing printing process when e.g. sheet by sheet with different layouts are needed. Recently inkjet technologies have been applied to electronics. In this field, the inkjet processes has been used for printable electronics and display manufacturing [29]. A typical inkjet printer used for printed electronics shown in Fig.4. This digital (variable information, customization), non impact printing process can print directly from computer data onto any substrate without any masks contrary to the traditional etching technique [1]. Inkjet printing jets the single ink droplet from the nozzle to the desired position; therefore almost no waste is created. It can also produce precise and high resolution with moderately fast. The combination of those drops makes a line pattern or area pattern freely according to a digital image designed. Metal (e.g. gold and silver) nano particles which are sintered to remove excess solvent in an oven at a temperature near 200 °C [5]. Electrical properties of the ink are mostly determined by conductive (silver) particles mixed and the way they connect in the cured ink. Printed electrical conductor has its resistance proportional to the overall trace length and be inversely proportional to the ink-layer thickness. Inkjet printing used in the manufacturing of electronics, MEMS (Micro Electro Mechanical systems), displays (LCD), RFID, solar cells, optics, diagnostics, medical science [19].

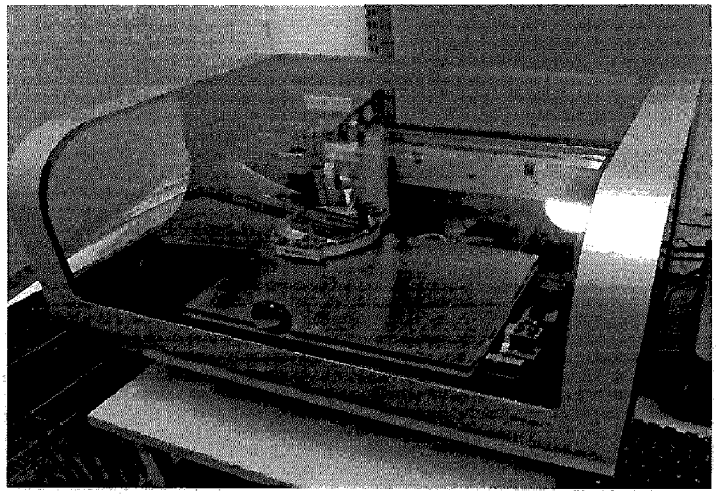

Fig. 4. Picture of ink jet printer used for printed electronics.

In practive two different inkjet printers are used: continuous and Drop On Demand (DOD) inkjet. In the continuous inkjet process, the droplet generator is made of a reservoir containing ink under pressure and undergoing a vibration [29]. The vibration increases the pressure inside the reservoir, which ejects a stream of fine droplets out of a nozzle. The droplets pass through a charged electrode and can then be reflected in two directions by two perpendicular electric fields. The droplets which are not to be printed are deflected into a gutter and recycled. The resolution is limited to 60 lines per centimeter, which remains rather low for printing electronics. In the DOD process [29], one single ink droplet can be jetted from the reservoir through the nozzle. This happens when the pressure within the reservoir increases, either due to the vibration of a piezo element (piezo system) or to a bubble resulting from the rapid evaporation of the heated ink

3.4. Parameter Analysis

The three essential parameters for the design of a L-shaped Monopole Antenna are:

- Frequency of operation (f_0): The resonant frequency of the antenna must be selected appropriately. The resonant frequency selected for design is 2.4 GHz.
- Dielectric constant of the substrate (ε_r): The dielectric materials used in the design are Rogers substarte 4003c with dielectric constant 3.38 , PPS sbustrate used for antenna design with dielectric constant 3.
- Height of dielectric substrate (h):The height of the dielectric substrate is selected as 0.83 mm

Hence, the essential parameters for the design are:

- f_0= 2.4 GHz
- ε_r = 3.38, 3
- h = 0.83 mm

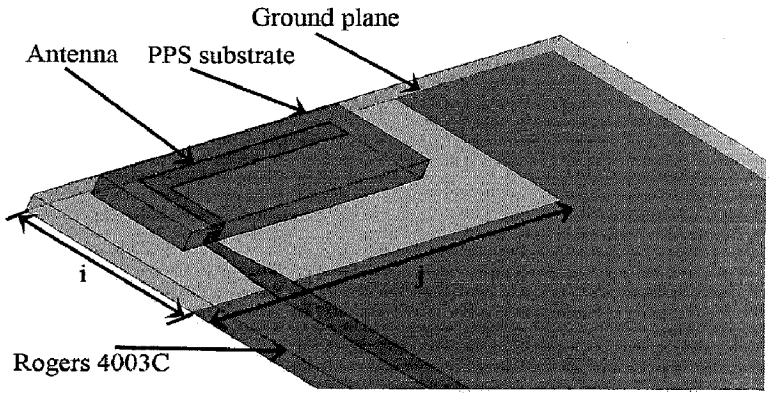

Fig. 5. A close view of the antenna structure.

Effect of antenna size :

The dimesion of antenna size is an important factor for achieving the resonant frequency. According to the theoretical calculations wavelength λ taken as 12.5 cm. For quarterwave Monopole the antenna size 31.5 mm. Using Ansoft HFSS v11 size of the antenna is optimized to achieve the the resonant frequency. Varying the antenna size is showing in Fig.6. When antenna size increasing resonant frequency is shifting from right to left side.

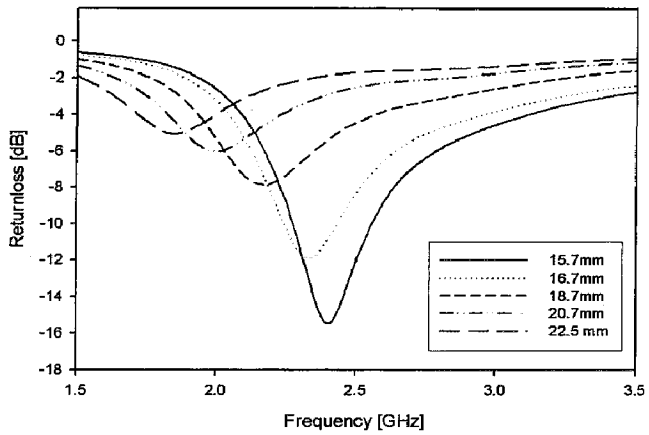

Fig. 6. Effect of size of the antenna

Effect of thickness of antenna substrate :

The effect of increasing thickness of substrate is shown in Fig. 7.

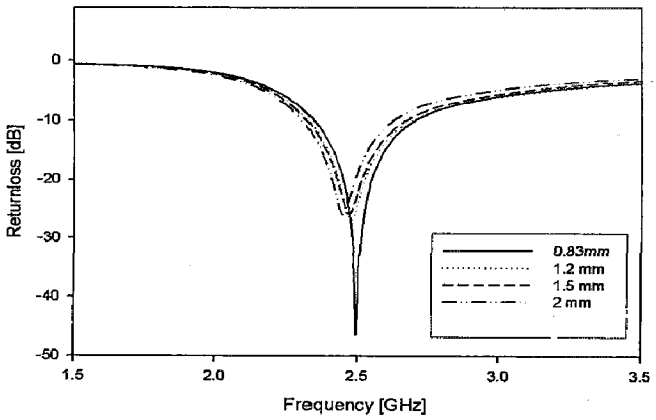

Fig. 7. Effect of thickness of substrate

Effect of geometrical parameters

In order to study the effect of the geometrical parameters (i and j) on the antenna return loss performance, the parameters were varied one at a time keeping the other fixed. The dimensions of the ground plane opening under the antenna element have been parametrically varied for optimizing the return loss performance of the antenna in 2.4 WLAN band. A close-up view of the antenna structure and the optimization parameters used, i. e. ground plane opening dimensions, i and j is shown in Fig. 5.The parametric analysis of the antenna has been performed using Ansoft HFSS (v.11).

Effect of i variation

Fig. 8 shows the dependence of the return loss as a function of i by keeping j as constant at 30 mm. As the value of i is increased from 5 mm to 20 mm, the resonant frequency shifts downwards and the impedance match improves. An optimum return loss of the antenna in the desired 2.4 WLAN band was achieved for i = 10 mm.

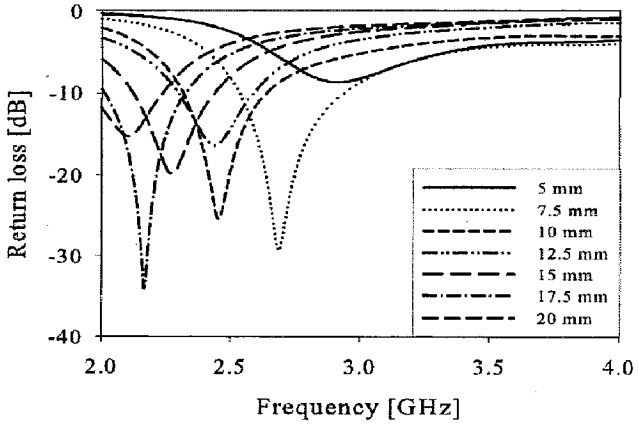

Fig. 8. Effect of i variation on the returnloss of the antenna.

Effect of j variation

As j is increased from 20 mm to 35 mm in steps of 2.5 mm and keeping i at 10 mm, a minimal upward shift in the resonant frequency and almost negligible shift with increase of j beyond 25 mm was simulated shown in Fig.9. A value of return loss better than -10 dB was obtained when j > 25 mm. Hence, an optimum values for i = 10 mm and j = 30 mm are chosen for the final design of the antenna which gives a return loss value better than -15 dB over 2.4 WLAN band (2.4 GHz – 2.484 GHz).

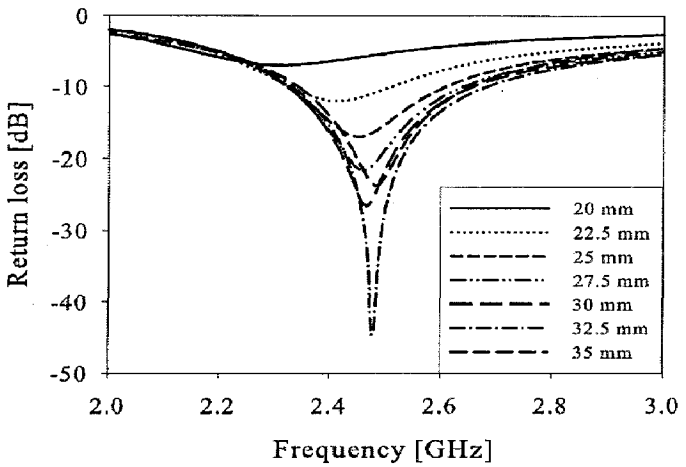

Fig. 9. Effect of j variation on the returnloss of the antenna shown in Fig.3.

4. Simulation and Measurement results

4.1. Simulation results

Ansoft HFSS is used to model and simulate the L-shaped monopole antenna, after which the simulation results model is verified by fabrication. This enables to evaluate the uncertainties in the measurements and therefore by comparing the simulated and measured reliable structure is obtained.

Simulation setup

Fig. 10 shows simulated return loss of the antenna. The return loss is an important measurement of an antenna, it tells how much impedance matching achieved. Adjusting the ground plane and antenna size return loss below -10 dB at 2.4 GHz was achieved. As shown the simulated returnloss is -24 dB at 2.44GHz. The simulated radiation pattern of the L-shaped monopole antenna using HFSS software is depicted in Fig.11.

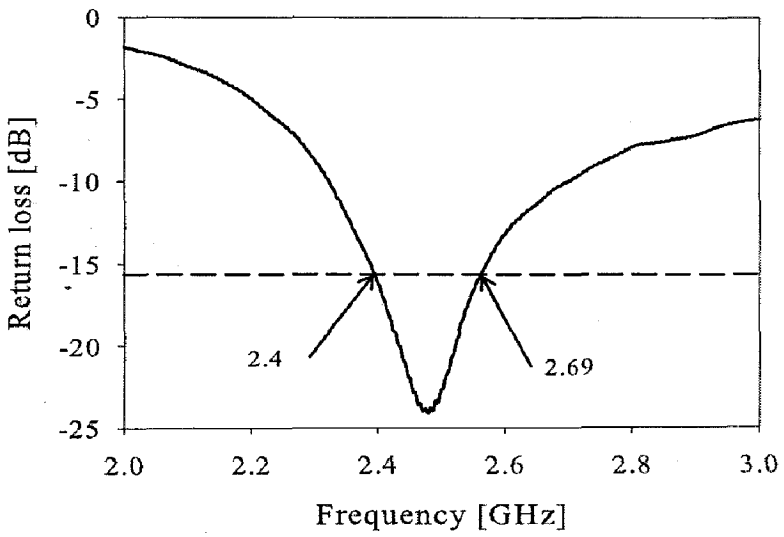

Fig.10. Simulated return loss of the L-shaped monopole antenna.

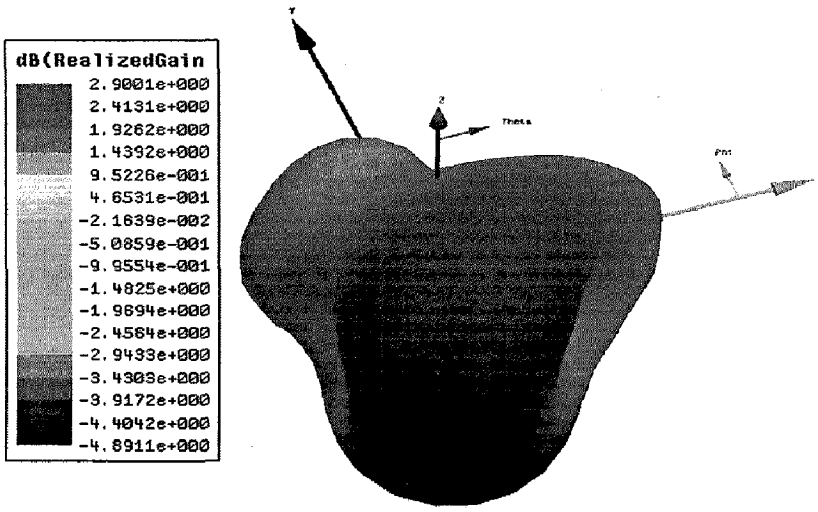

Fig. 11. Simulated radiation pattern of the L-shaped monopole antenna.

4.2. Measurement results of reference antenna

Designed L-shaped monopole antenna was fabricated with two different methods, by etching on the copper coated Roger substrate 4003C and by inkjet printing on PPS substrate. The antenna fabricated with copper is taken as a reference antenna. The thickness of Roger substrate and PPS substrate was about 0.83 mm. In both cases, the lower substrate is fixed as Rogers.

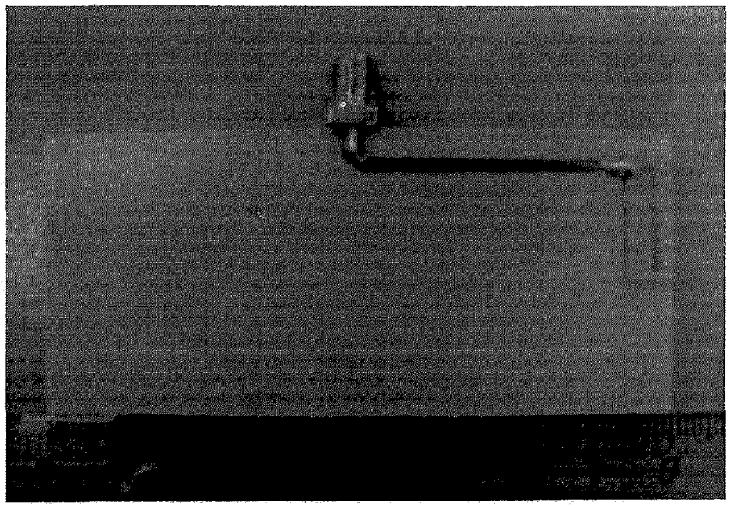

Fig. 12. Picture of the fabricated L- shaped monopole reference antenna.

The conductive connection between the antenna and the microstrip feed was made by using conductive epoxy, which was heated to 125 °C for 15 minutes. Copper laminate on the Roger substrate was approximately 20 μm thick. The fabricated reference antenna is shown in Fig.12. The return loss of the fabricated antennas were measured and compared to the simulated results. The optimized design is prototyped and experimentally verified using HP 8720ES Network analyzer. The return loss was measured in radio anechoic room. The efficiency and gain of the antenna were measured with Satimo Starlab measurement system as well as the radiation pattern.

4.2.1. Return loss

The return loss is usually the first parameter measured when prototype antenna since it shows the frequency, impedance matching and bandwidth of the antenna. These parameters tell if modifications are required in the design before further measurements. Fig. 13 shows the measured return loss of the L-shaped monopole antenna made on the Rogers substrate. This antenna takes as reference antenna. The antenna covers the required WLAN 2.4-2.484 GHz with less than -16 dB return loss being -24 dB at center frequency of 2.425 GHz

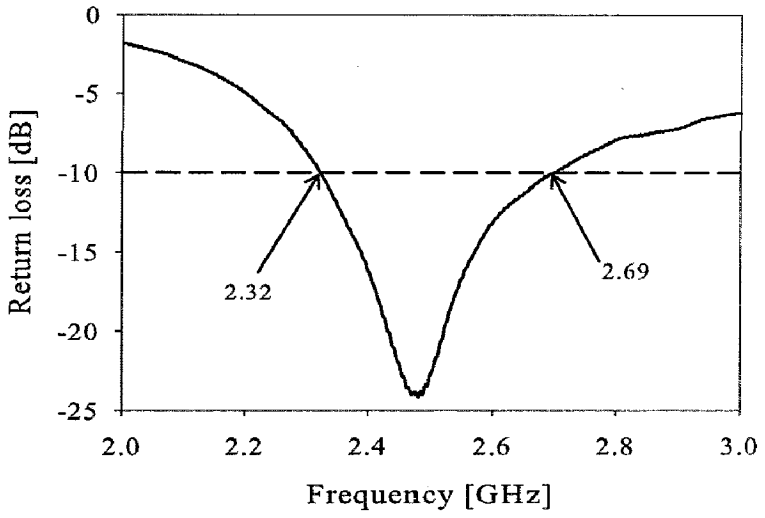

Fig. 13. Measured returnloss of the reference antenna.

4.2.2. Satimo StarLab Measurement system

Satimo StarLab is the ultimate tool for antenna measurements in laboratories and production environment, where space is limited, cost is critical and the flexibility of a movable system required. Satimo Starlab measurement equipment [30] shown in Fig. 14. StarLab uses a switching unit to switch between passive and active measurements RF instrumentation. For passive measurements, a vector network analyzer is used as the RF source/receiver for antenna measurements. The control unit drives the two positioning motors and the electronic scanning of the probe array. For active measurements the test is performed through a Multi Protocol Radio Communication Tester. Amplification units are added on both transmission and receiver chains. Starlab can perform the following measurements.

- Gain, directivity, 3D radiation pattern, beam width, cross polar discrimination, sidelobes.
- Radiation pattern in any polarization, linear or circular, as well as antenna efficiency.

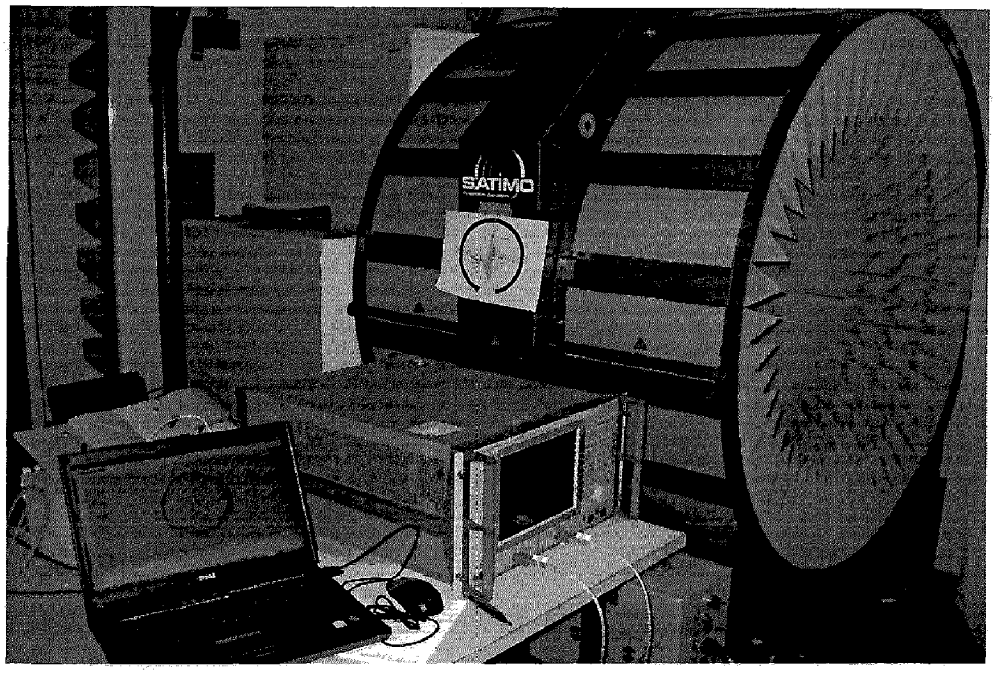

Fig. 14. Picture of the Satimo starlab measurement system for the measurement of the Antenna performance.

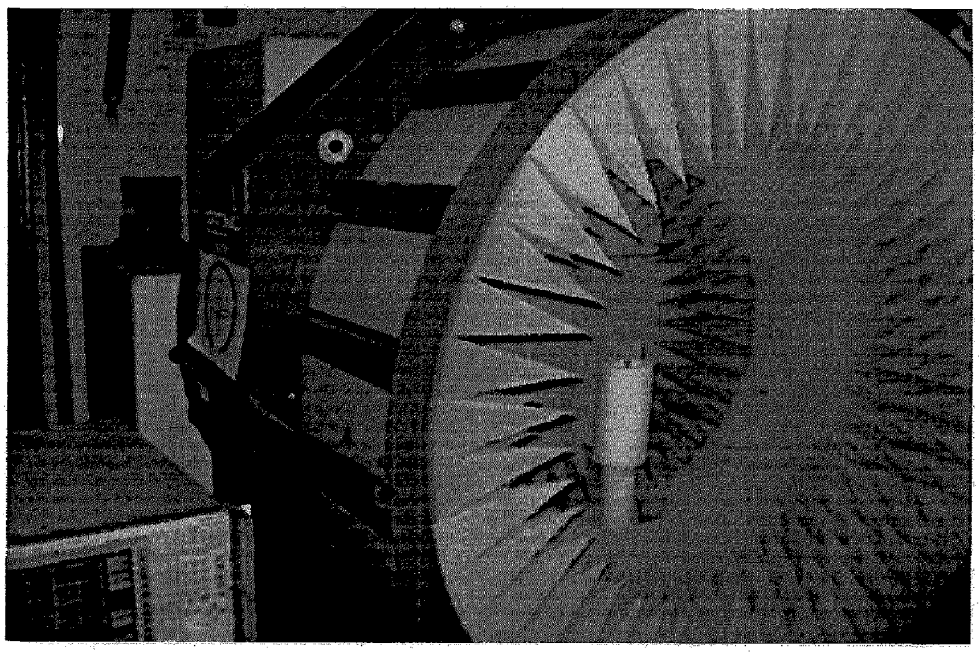

Fig. 15. Placement of DUT in the starlab

The Satimo chamber has fifteen measuring probes on the inner circle of the chamber. StarLab test station is connected to a PC that controls all the equipment (probe array, azimuth and elevation motors, RF source and RF measurement devices) through a light version of the software environment called SatEnv shown in Fig. 16.

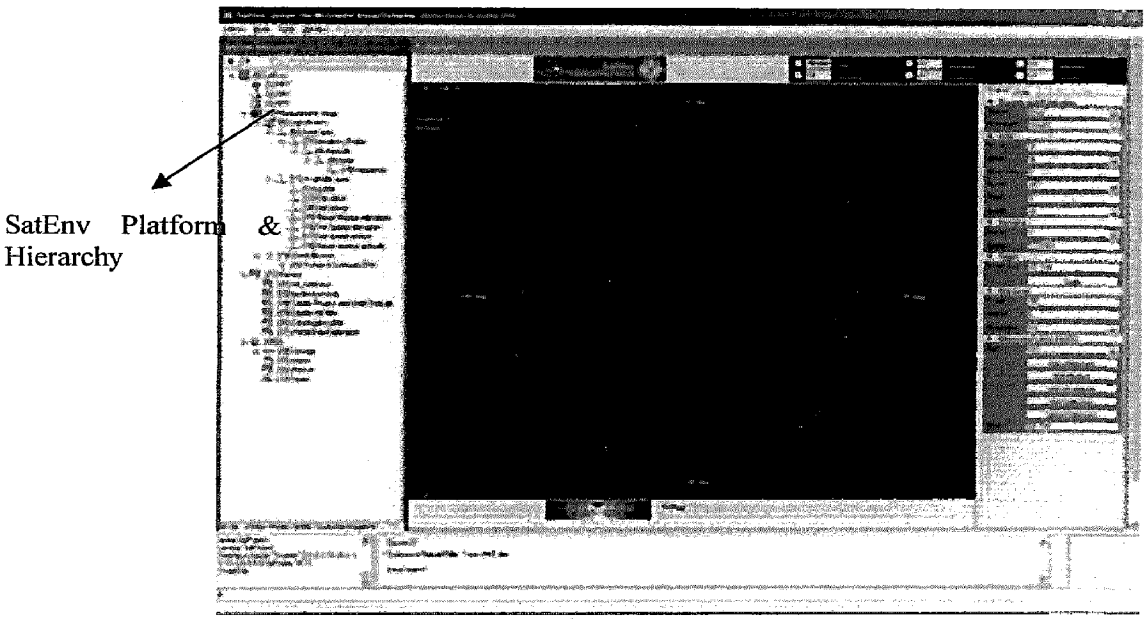

Fig. 16. SatEnv software used for passive measurements

The software also performs the acquisition, the post processing and the visualization of the measurement data.The user can see in real time the radiation pattern of the

measured device expressed in radiated power or gain. (1-D pattern cuts in Cartesian or polar format, 2-D data plots or 3-D plots). The far-field of the antenna is calculated by Satenv-measurement software which use Fourier transform to convert the far-field from measured near-field. Satimo uses circular probe array to allow for real time elevation cuts and volumetric 3D radiation measurements. Spacing between the probes are 22.5°. These probes contain a pair of orthogonal printed antennas designed to provide broadband characteristics. The DUT is located at the center rotated by a motor to sample the radiationfield over the full sphere surrounding the DUT. Radiation pattern can be measured in three dimensions and the results are presented in three cuts which are Phi 0°, Phi 90° and Theta 90°. These cuts can be seen in Appendix 1. The manufacturer announces the accuracy of the measurements to be ± 0.8 dB at frequency 1-6 GHz and the accuracy of measurements repeatability is ± 0.3 dB.

4.2.3. Total Efficiency

Total efficiency, which tells how much of power fed to antenna is radiating to the air, is measured with Satimo measurement system. The result for the reference antenna is shown in Fig. 17. The reference antenna showed measured maximum efficiency of 90 % and in the frequency range of 2.3 – 2.6 GHz it has 75 % total efficiency

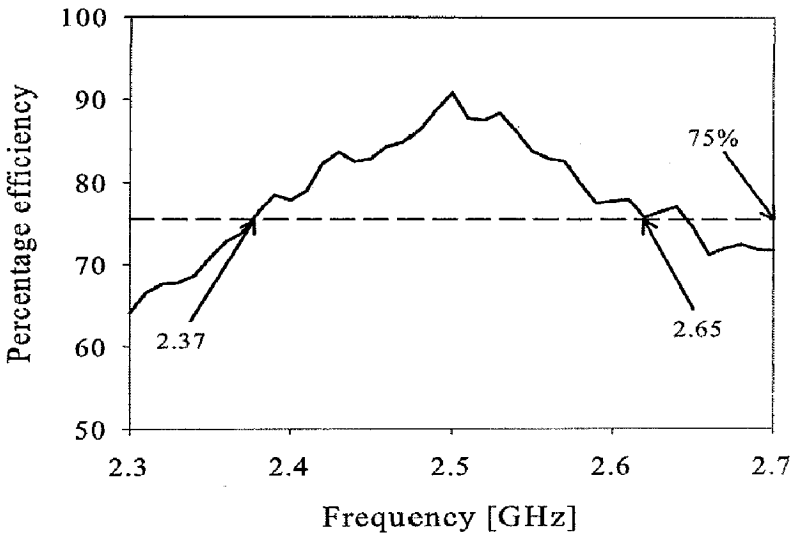

Fig. 17. Measured total efficiency of L-shaped monopole reference antenna.

4.2.4. Total Gain

The total gain which is the sum of partial gains is measured with Satimo StarLab measurement system. Fig. 18 represents the total gain of L-shaped monopole reference antenna. The maximum peak gain measured in free space is 2.2 dB at 2.43 GHz frequency.

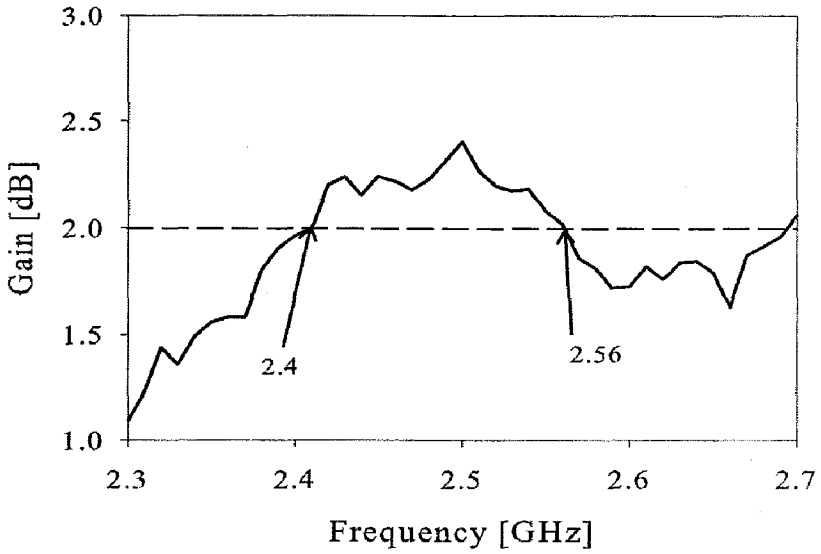

Fig.18. Measured gain in dB of L-shaped monopole reference antenna.

4.2.5. Radiation pattern

A graphical representation of the relative distribution of the radiated power in space is called a radiation pattern. The radiation pattern describes the relative strength of the radiated field in various directions from the antenna at a fixed distance. Often the radiation patterns are measured using slices of the three-dimensional pattern. Fig. 19 represents the measured radiation patterns of the reference antenna. The radiation pattern is measured with Satimo measurement system and the graphs shown are standard cuts at Phi 0°, Phi 90° and Theta 90° which represent X-Z, Y-Z and X-Y planes, respectively. These planes are situated in spherical polar coordinate system. The figure of planes can be seen in Appendix 1. The measured results show that the radiation patterns of the reference antenna are almost omnidirectional

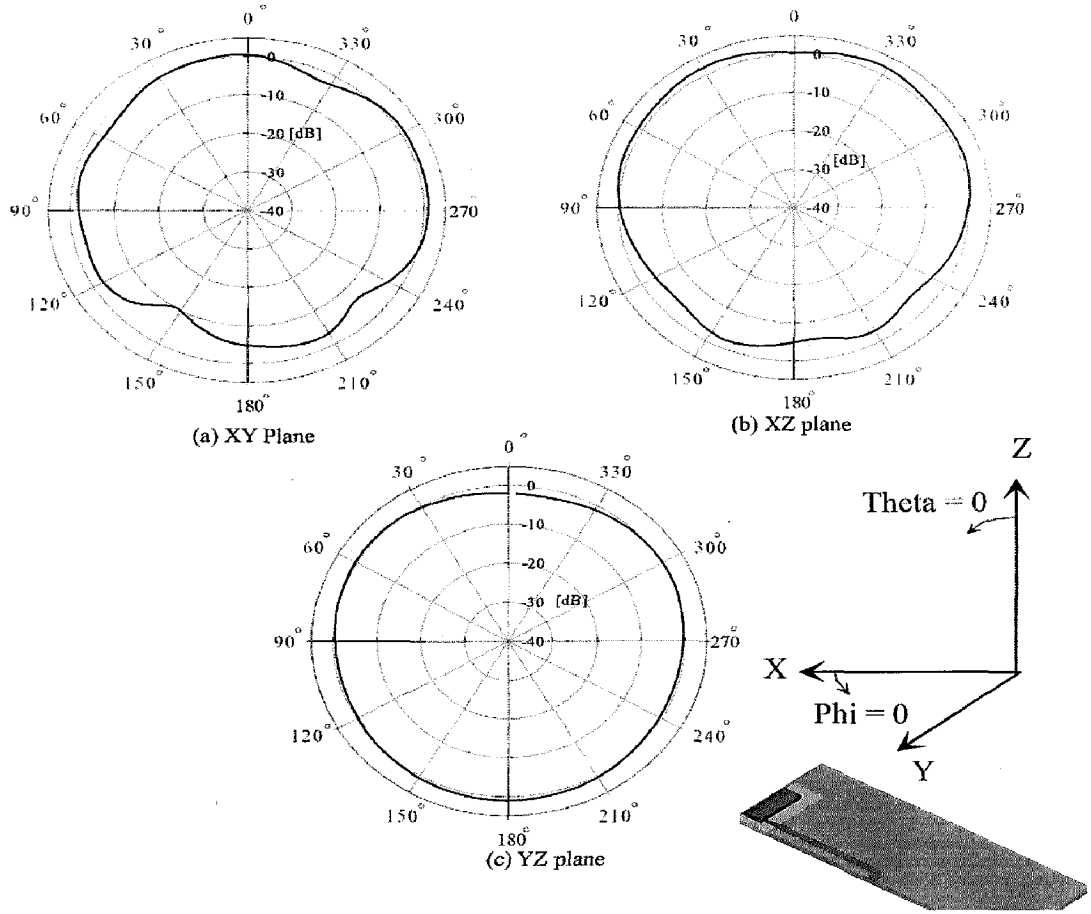

Fig. 19. Measured far-field radiation patterns of the reference antenna (a) in the XY plane , (b) in the XZ plane, (c) in the YZ plane.

4. 3. Measurement results of the inkjet silver printed L-shaped monopole antennas with different conductor thickness

The efficiency, gain and radiation patterns of the inkjet silver L-shaped monopole antenna were measured with Satimo Starlab measurement system.

4. 3.1 . Measurement of inkjet sliver conductor width and thickness

Fig.20 shows the fabricated L-shaped monopole antenna printed by depositing nano silver ink (Harima Chemicals Inc., Japan, NPS-J) with an inkjet printer on PPS substrate [31]. The thickness of printed ink- jet silver layer was measured by using Microscope and the software is Cell A image software , after focusing the antenna with 50X, take the snapshot of that antenna. Next go to measurements and took the arbitrary distance measurement. For measuring the cross section of antenna conductor thickness, first made the samples according to the following procedure. Mix the correct amount of hardener into the correct amount of resin. For each

sample, mix resin 7.5 ml (8. 33 g) with hardener 1ml (1g). By volume use the syringes to measure out the exact amount. Stir the mixture well for approx. 2 min without introducing too many air bubbles. Leave to rest for 2 minutes and pour the epoxy carefully over the specimen. Curing is 12 hours.Fig. 21. Shows the top view of the inkjet printed conductor lines with thickness of 4.5 μm (four printings).

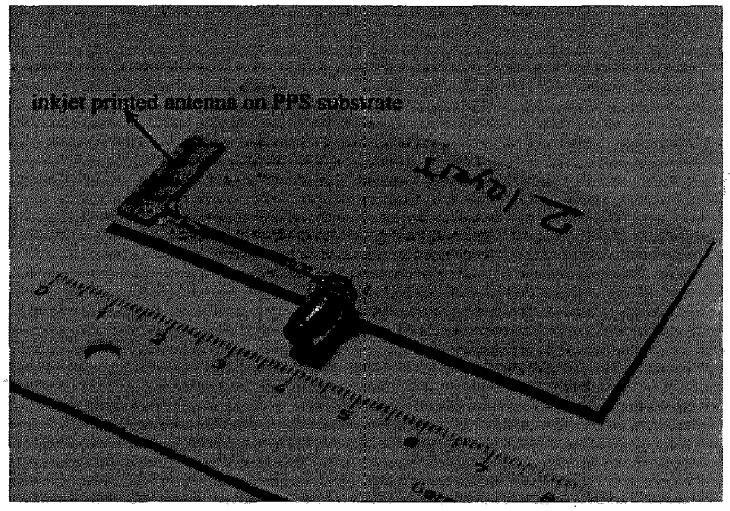

Fig. 20. Fabricated inkjet printed L-shaped monopole antenna.

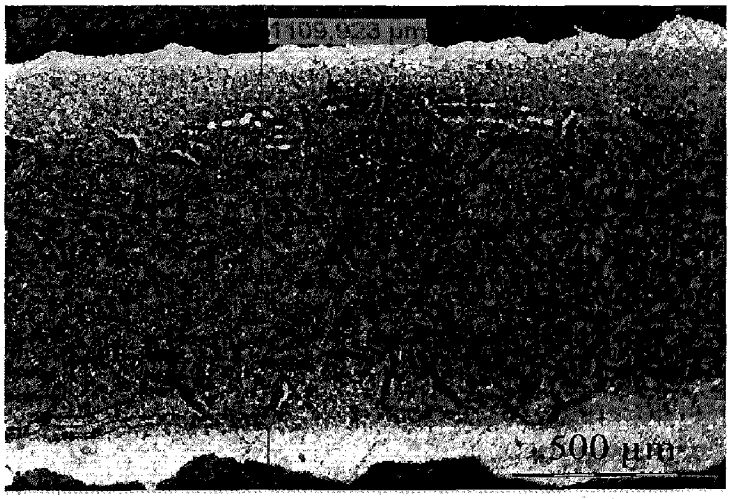

Fig. 21. Top view of the conductive line after four inkjet printings.

Cross section of L shape monopole antenna conductor printing (1.5 μm) on PPS substrate is shown in Fig. 22. Fig. 23 shows the width of fabricated copper L-shaped monopole reference antenna on the Rogers 4003 C substrate . The average width measured is 880 μm. Cross section measurements of Copper L-shaped monopole reference antenna (Fig. 22) showed thickness of approximately 20.5 μm.

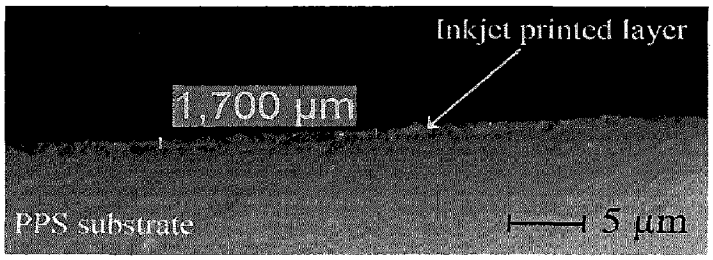

Fig. 22. Cross section of printed 1.5μm thickness

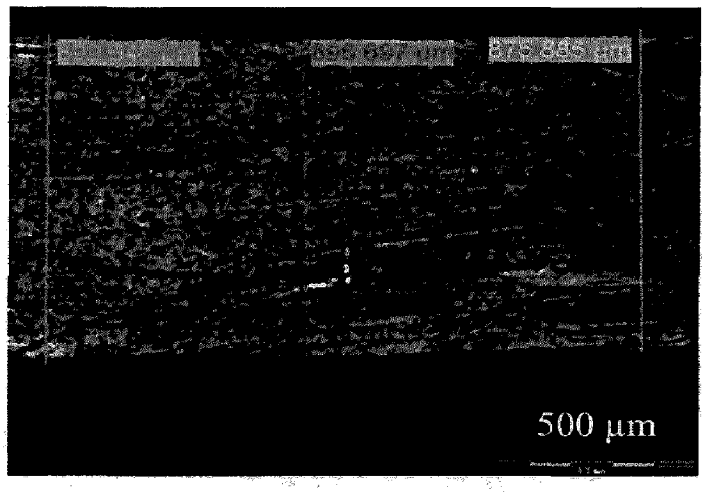

Fig. 23. Width Measurement of copper L-shaped monopole reference antenna

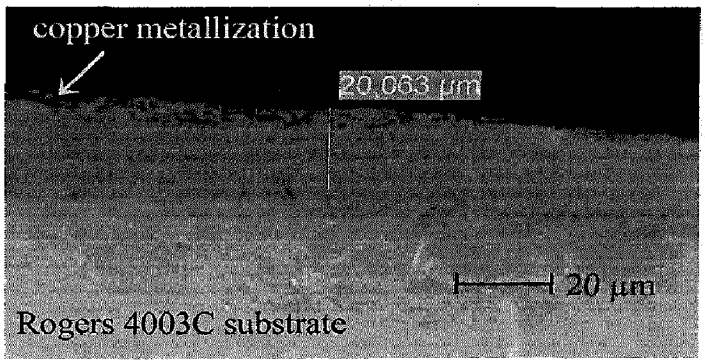

Fig. 22. Cross section of the reference antenna.

Table 1. Measurement thickness of inkjet printed L-shaped monopole antenna after 1-5 printings.

Layer number	Thickness [μm]
1 layer	1.5
2 layer	2.5
3 layer	3.5
4 layer	4.5
5 layer	5.5
reference	20.5

4.3.2. Returnloss

Fig.23. shows the return loss of the L-shaped monopole antenna with printed layer thicknesses from 1.5 to 5.5 μm (1-4 printings) on 0.83 mm thick PPS substrate and the return loss of the reference antenna. At 2.43GHz the return loss is -28.36 dB when the conductor layer was printed once producing thickness of 1.5 μm. The antenna covers the required WLAN 2.4-2.484 GHz with less than -18 dB. With further printings the return loss clearly improved. The return loss at whole frequency band for 2-4 printings were -21 dB, -20 dB and -14 dB, respectively, as the thickness of the conductive layer increases from 3.5 μm to 5.5 μm.

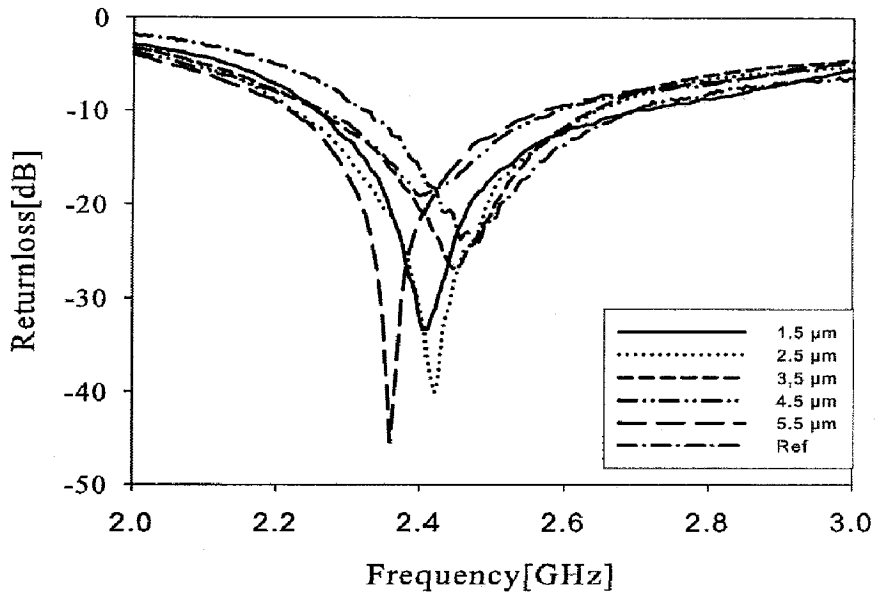

Fig.23. Measured return loss of inkjet printed L-shaped monopole antenna with different printed layer thickness.

Finally the return loss of the monopole antenna with five printed layers (5.5 μm thickness) shows measured return loss measured of -17.4 dB at 2.43 GHz an the antenna covers the required WLAN 2.4-2.484 GHz with less than -13 dB. The results show that the printed antenna has very competitive return loss properties when compared to the reference antenna with laminated copper having thickness of 20 μm.

4.3.3. Total efficiency

Fig. 24 shows the efficiency of the printed antennas with different silver conductor thickness and the performance of the reference antenna as a comparison. The total efficiency with 1.5 μm silver conductor thickness is 59 %. In this case also increase of the conductive material thickness (more printings) improved the performance. The total efficiency with the thickness of 2.5 μm, 3.5 μm, 4.5 μm and 5.5 μm showed values of 65 %, 79 %, 85 % and 88 %, respectively

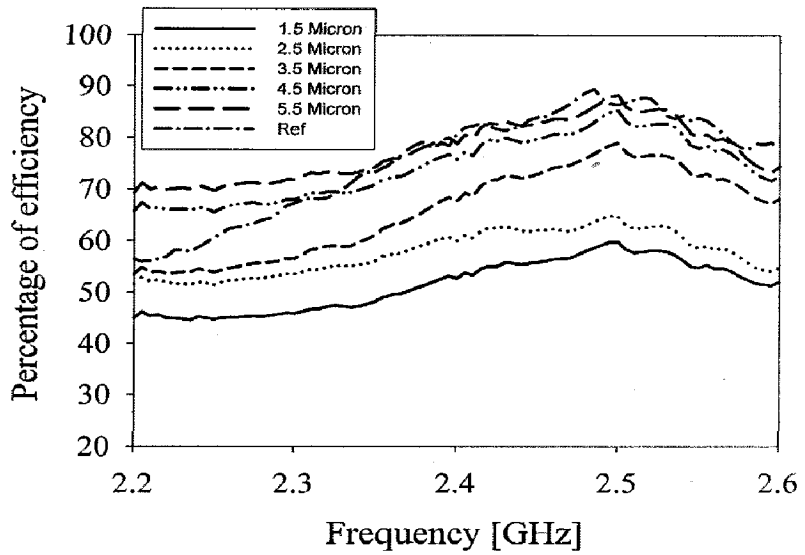

Fig. 24. Measured total efficiency of the ink-jet printed L-shaped monopole antenna with different layers.

The achieved indicates that the inkjet printing is able to produce competitive antenna structure since the reference antenna using copper foil showed total efficiency of 90 %.

Table 2. Measurements total efficiency for inkjet printed L-shaped monopole antenna with different silver conductor thicknesses.

Layer thickness [μm]	Efficiency [%]
1.5	59
2.5	65
3.5	79
4.5	85
5.5	88

4.3.4. Total Gain

The total gains of the different silver conductor thickness of L-shaped monopole antennas are measured with Satimo StarLab measurement system. Fig. 25 shows the gains of L shape monopole antenna with different silver conductor thicknesses as well as the the total gain for the reference antenna.

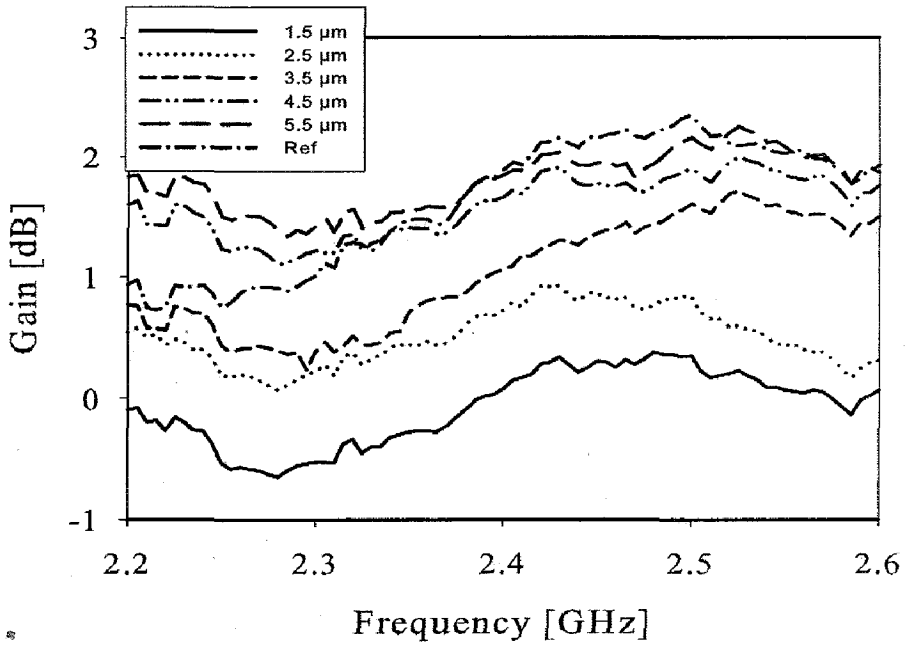

Fig. 25. Measured gain for the inkjet printed L-shaped monopole antenna with different conductor thicknesses.

The maximum peak gain after one printing (1.5 μm thickness) is 0.3 dB at 2.45 GHz frequency. More printings clearly improved the gain as shown in Table 3 and after five printings with thickness equal to 5.5 μm shows the maximum gain of 1.96 dB. The reference antenna had maximum gain of 2.2 dB.

Table 3. Measured gain of inkjet printed L shape monopole antenna with different silver conductor thicknesses.

Layer thickness [μm]	Gain [dB]
1.5	0.30
2.5	0.85
3.5	1.38
4.5	1.75
5.5	1.96

4.3.5. Total Radiation pattern

Fig. 26. shows the radiation pattern cuts in Phi 0°, Phi 90° and theta 90° for the L-shaped monopole antenna after 1-5 conductor printings. The antenna has omni directional radiation pattern in free space as achieved also to the reference antenna (Fig. 19) without large difference.

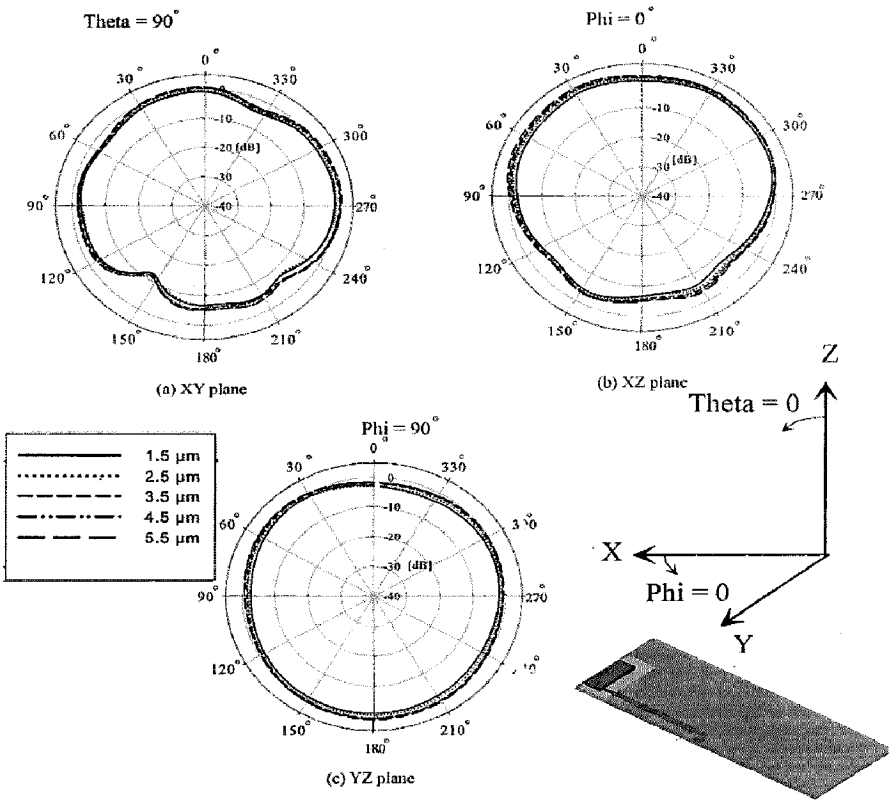

Fig.26. Measured far-field radiation pattern of the inkjet printed monopole antenna with different conductor thickness a) in the XY plane b) in the XZ plane c) in the YZ plane.

5. Conclusion and Future work

In this thesis, the L-shaped monopole antenna is designed and fabricated with different printed silver conductor layer thickness from 1.5-5.5 μm. The electromagnetic simulations were performed with Ansoft HFSS modeling software. The antenna modeling, fabrication and the results were presented. The fabrication methods were inkjet printing on the PPS substrate and etching on the copper coated Roger substrate. The effect of increasing inkjet printed silver layer thickness on the antenna performance was studied. The results show that when the conductor layer thickness is low compared to the skin depth the antenna performance, that is the return loss, gain or efficiency, does not reach to required performance values. It should be noted that the skin depth at 2.5 GHz with bulk silver electrodes is 1.5 μm. This is the thickness reached with one printing. However as mentioned earlier, the optimum performance needed conductor thickness of about skin depth multiplied with 3-4. This means thickness of 4.5-6 μm for the proposed antenna with center frequency of about 2.4 GHz. The results confirm this. They actually show that 4-5 printings are needed to reach the same antenna performance as measured for the reference antenna with copper foil of 20 um. This is clearly seen in Fig. 27 where the peak total efficiency of the antenna increases with the printed layer thickness.

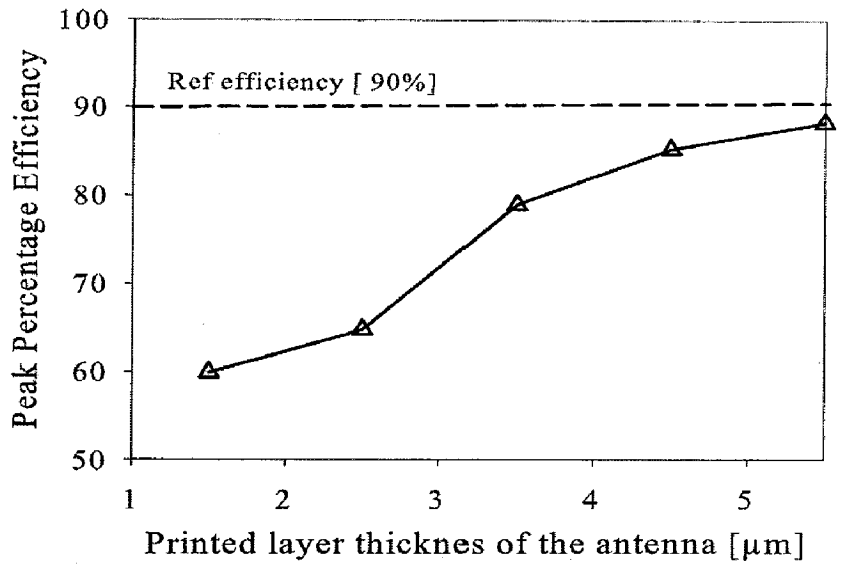

Fig. 27. Measured peak total efficiency of the inkjet printed L- shaped monopole antenna as a function of printed silver conductor thickness.

Fig. 28 shows also that the peak gain approaches to the peak gain of copper reference antenna when the thickness of the printed conductor increases. With inkjet silver layer thickness 5.5 μm of 5 layers has 1.96 dB gain and thus almost meets required 2 dB gain.

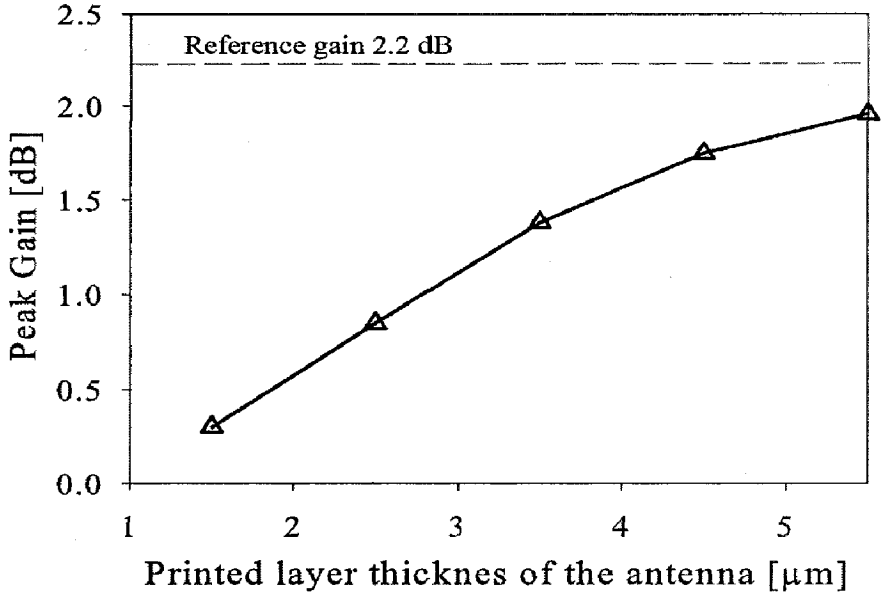

Fig.28. Measured peak gain of the inkjet printed L-shaped monopole antenna as a function of printed silver conductor thickness

The main purpose of this thesis was to find the performance of antenna with varying silver conductor layer thickness and find for which thickness, performance is reaching closer to performance of copper. For silver layer thickness of 5.5 μm achieved the closer to copper thickness 20 μm antenna performances.

As a conclusion this thesis clearly shown that the modern printed electronics technique using inkjet printing is able to produce wireless telecommunication devices with very competitive manner. The conductivity of the silver nano ink as well as the accuracy of the printing method itself seems to be good enough for practical applications and only thing one must consider is the thickness of printed areas. With the materials used in this thesis, the optimum thickness is about 4 times the skin depth theoretically calculated for bulk silver.

Finally during the work some observations beneficial for the research might be explored in future. The printing of different type of antenna structures on different substrates could be considered in future. In inkjet printing not only silver ink solvents but also other conductive inks (copper) might be used to reduce the cost of printing. For achieving good performance parameters of antenna printed layer thickness around 5.5 μm is sufficient.

Candidate's Publications

1. Arun kumar Sowpati, Vamsi Krishna Palukuru, Vesa Pynttäri, Riku Mäkinen, M. V. Kartikeyan, and Heli Jantunen, " Performance of Printable Antennas With Different Conductor Thickness" International Journal on Progress in Electromagnetic Research (PIER). *(Under Review)*

2. Arun kumar Sowpati, Ashwin K Arya and M. V. Kartikeyan, "Proximity Coupled Dual Frequency Microstrip Antenna for WLAN" Proceeding Symposium on Vaccum Electronic Devices and Applications (VEDA-2009), pp. Ant. 2-1 to Ant. 2-3, 2009.

3. Arun kumar Sowpati, Vamsi Krishna Palukuru, M. V. Kartikeyan, and Heli Jantunen, " Performance of Printable Antennas With Different Conductor Thickness" 16th International Student Seminar on Microwave and Optical Applications of Novel Phenomena and Technologies, University of OULU, Oulu, Finland, 8th – 9th June, 2009.

References

1. Rida A, Vyas R, Li Y, Kruesi C & Tentzeris MM (2008) Low cost inkjet-printing paper-based modules for RFID sensing and wireless applications. Proc. European Conference on Wireless Technology, 27-28: 294-297.

2. Siden, Fein MK, Koptyug A & Nilsson HE (2007) Printed antennas with variable conductive ink layer thickness. IET Microwaves, Antennas & Propagation 2: 401-407.

3. Li Y & Vyas R (2007) RFID Tag and RF Structures on a Paper Substrate Using Inkjet-Printing Technology. IEEE Transactions on Microwave theory and techniques 55(12): 2894-2900.

4. Siden J & Nilsson HE (2007) Line width limitations of flexographic-screen- and inkjet printed RFID antennas. IEEE Antennas and Propagation Society International Symposium. Honolulu, HI, USA: 1745-1748.

5. Mantysalo M & Mansikkamaki P(2007) An inkjet-deposited antenna for 2.4 GHz applications. International Journal AEU of Electronics and Communications 63: 31-35.

6. Rida, A, Li Y & Tentzeris MM (2007) Design and characterization of novel paper-based inkjet-printed UHF antennas for RFID and sensing applications. IEEE Antennas and Propagation Society International Symposium. Atlanta, USA: 2749-2752.

7. Marko P, Niina H, Paivi G & Jouko V(2005) Gravure printing of conductive particulate polymer inks on flexible substrates. Progress in Organic Coatings 54: 310-316.

8. A Koptioug, Jonsson P (2003) On the behavior of printed RFID tag antennas using conductive paint. Proceedings of Antenna-03, Sweden.

9. Merilampi S, Ukkonen L & Ruuskanen (2007) Analysis of silver ink bow-tie RFID tag antennas printed on paper substrates. International Journal of Antennas and Propagation 90762: 1-9.

10. Li Y, A Rida, Terence Wu & Serkan B (2007) Integration of Sensors and Inkjet-printed RFID Tags on paper-based substrates for UHF "cognitive intelligence" Applications. IEEE Antennas and Propagation Society International Symposium : 1193-1196.

11. Huebner G & Ingmar P Printed antennas for automotive applications. www.hdmstuttgart.de/international_circle/circular/issues/08_01/ICJ_01_35_huebner_petersen.pdf

12. Jolke P, Patrick J & Erwin V (2009) Spreding of inkjet printed droplets with varying polymer molar mass on a dry solid substrate. Macromol. Chem. Phys 210 : 495-502.

13. Tentzeris M & Rida A (2009) Inkjet printing of green RFID and RFID enabled sensors on flexible substrates. IMS 09. http://www.ims2009.org/pdfs/workshop/WFA/WFB.pdf.

14. Sridhar A and Akkerman R Characterisation of the interface between inkjet printed components and substrate materials. http://www.schubert-group.de/PDF/IJWorkshop/IJ_Sridhar.pdf

15. Eloi R, Jordi M and Cristina C Inkjet printed on organic substrates. http://www.athena-gatech.org/papers/yang3.pdf.

16. Prabir k, Paul D & Dayalan K Textile based carbon nano structured flexible antenna. http://www.ntcresearch.org/pdf-rpts/Bref0607/M06-MD01-07.pdf

17. Palukuru V, Pekonen A & Pynttari V (2009) An inkjet printed inverted-F antenna for 2.4 GHz wrist applications. Microwave and optical technology letters 51(12) : 2936-2938.

18. Jolke P, Klokkenburg M, Hendriks C (2009) Microwave flash sintering of inkjet printed silver tracks on polymer substrates. http://www.scribd.com/doc/18577757/Microwave-Flash-Sintering-of-InkjetPrinted-Silver-Tracks-on-Polymer-Substrates

19. Shin D, Lee Y & Kim C (2009) Performance characterization of screen printed radio frequency identification antennas with silver nanopaste. Thin solid films 517 : 6112-6118.

20. Tovia F & Ujiie H (2007) Creation of Textile-Based Durable Printed Antenna Systems. http://www.hitoshiujiie.com/inkJet/proposed06/M07-PH05.pdf.

21. Balanis CA (1997) Antenna Theory – Analysis and Design. Second edition, John Wiley & Sons, New York

22. Stutzman WL & Thiele GA (1998) Antenna Theory and Design. Second edition, John Wiley & Sons, New York, p.941

23. Collin RE (1992) Foundations for microwave engineering. Second edition, McGraw-Hill, p. 329.

24. Pozar DM (1988) Microwave Engineering. Second Edition, John-Wiley & Sons, p.19-21.

25. Daniel G, Swanson Jr, Wolfgang J. R. Hoefer , Microwave Circuit Modeling Using Electromagnetic Field Simulation Artech House, pp.125-127.

26. Datasheet for Rogers 4003C . Online (2009) Cited September 11th from www. rogerscorp.com/acm/literature.aspx

27. Hu T, Juuti J, Jantunen H (2006) RF properties of BST-PPS composites. European Ceramic society 27: 2923-2926.

28. Datasheet for polyphenylene sulfide. Online (2009) Cited August 14th from http://www.schafferprecision.com/machining/materials/tecatron_p.htm.

29. Birkenshaw J (2004) Printed Electronics. PIRA International: 80.

30. Satimo Starlab training user manual (2006): 22.

31. Datasheet for hurjuma INS-J type ink URL:

http://www.harima.co.jp/en/products/electronics/pdf/GB_E_0612_EM_11_NP.pdf [cited 14.09.2009]

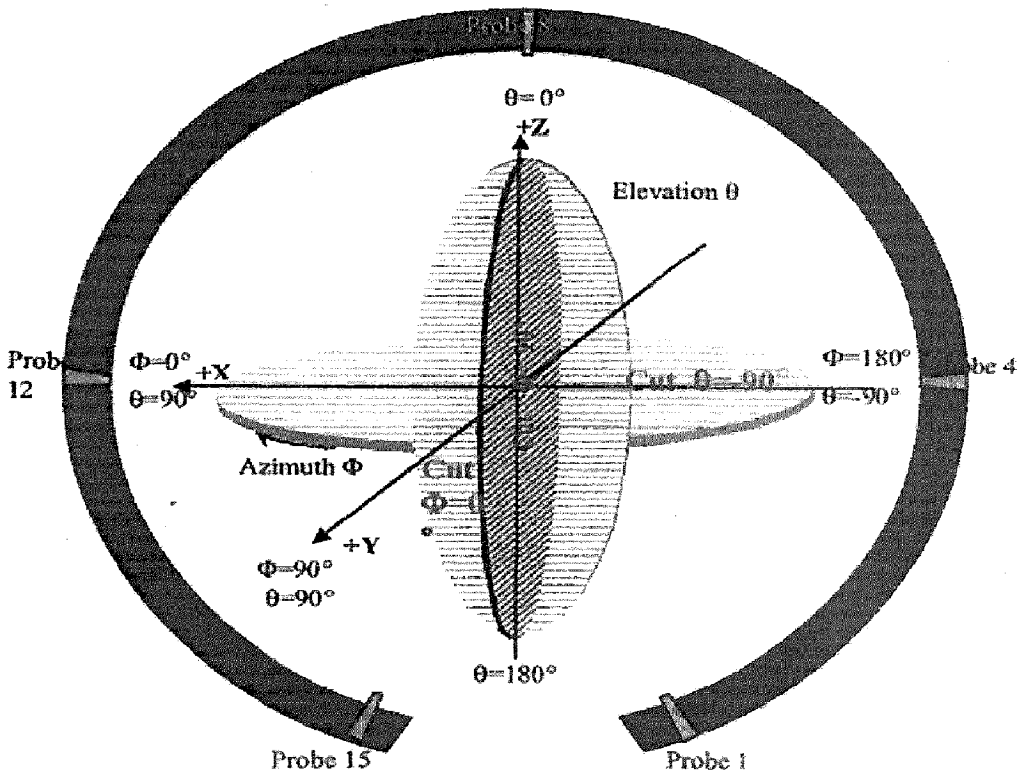

Appendix 1. Placement of the measured antenna in Satimo starlab 3D space.

ABBREVIATIONS AND VARIABLES

BW	bandwidth [Hz]
EM	electro magnetic
SMA	sub miniature version A
UHF	ultra high frequencies 300-3000 MHz
VHF	very high frequencies 30-300 MHz
VSWR	voltage standing wave ratio
D	directivity
d	largest dimension of the antenna
E	electric field [V/m]
e_c	conduction efficiency [%]
e_d	dielectric efficiency [%]
e_o	total efficiency [%]
e_r	reflection efficiency [%]
f	frequency [Hz]
G	gain [dB]
I	the current fed to the antenna input [A]
k	wave number
P_{in}	the input power accepted by the antenna [W]
P_l	power loss per second in the system [W]
P_{rad}	total radiated power [W]
R_A	input resistance [Ω]
R_l	loss resistance of the antenna [Ω]
RL	return loss [dB]
R_{loss}	ohmic losses [Ω]
R_r	radiation resistance [Ω]
U	maximum radiation intensity in the direction of main beam [W/ unit solid angle]
X_A	power stored in the near field of antenna [W]
Z_A	input impedance [Ω]
Z	load impedance [Ω]
Z_0	nominal impedance [Ω]
ε_r	relative permittivity
e_{cd}	antenna radiation efficiency [%]
λ	wave length [m]
λ_0	free space wavelength [m]
ρ	power reflection coefficient
ρ_l	voltage reflection coefficient
σ	conductivity [S/m]
ω	rotation at radian frequency [rad]
ω_r	angular resonant frequency [Hz]
θ	elevation 0-180°
φ	azimuth 0-360°
δ	skin depth